Inorg. Chem. **2006**, *45*, 8108–8119

Syntheses and X-ray Crystal Structures of Zirconium(IV) and Hafnium(IV) Complexes Containing Monovacant Wells–Dawson and Keggin Polyoxotungstates

Chika Nozaki Kato, Akira Shinohara, Kunihiko Hayashi, and Kenji Nomiya*

Department of Materials Science, Faculty of Science, Kanagawa University, Hiratsuka, Kanagawa 259-1293, Japan

Received April 18, 2006

The syntheses and crystal structures of a series of zirconium(IV) and hafnium(IV) complexes with Dawson monovacant phosphotungstate $[\alpha_2\text{-}P_2W_{17}O_{61}]^{10-}$ and in situ-generated Keggin monovacant phosphotungstate $[\alpha\text{-}PW_{11}O_{39}]^{7-}$, which was obtained by a reaction of $[\alpha\text{-}PW_{12}O_{40}]^{3-}$ with Na_2CO_3, are described. $K_{15}H[Zr(\alpha_2\text{-}P_2W_{17}O_{61})_2]\cdot 25H_2O$ (K-**1**), $K_{16}[Hf(\alpha_2\text{-}P_2W_{17}O_{61})_2]\cdot 19H_2O$ (K-**2**), $(Et_2NH_2)_{10}[Zr(\alpha\text{-}PW_{11}O_{39})_2]\cdot 7H_2O$ (Et_2NH_2-**3**), and $(Et_2NH_2)_{10}[Hf(\alpha\text{-}PW_{11}O_{39})_2]\cdot 2H_2O$ (Et_2NH_2-**4**), being afforded by reactions in aqueous solutions of monolacunary Dawson and Keggin polyoxotungstates with $ZrCl_2O\cdot 8H_2O$ and $HfCl_2O\cdot 8H_2O$ followed by exchanging countercations, were obtained as analytically pure, homogeneous colorless crystals. Single-crystal X-ray structure analyses revealed that the Zr(IV) and Hf(IV) ions are in a square antiprismatic coordination environment with eight oxygen atoms, four of them being provided from each of the two monovacant polyanion ligands. Although the total molecular shapes and the 8-coordinate zirconium and hafnium centers of complexes **1**–**4** are identical, the bonding modes (bond lengths and bond angles) around the zirconium(IV) and hafnium(IV) centers were dependent on the monovacant structures of the polyanion ligands. Additionally, the characterization of complexes **1**–**4** was accomplished by elemental analysis, TG/DTA, FTIR, and solution (^{31}P and ^{183}W) NMR spectroscopy.

Introduction

The coordination chemistry of polyoxometalates with group 4 elements has attracted considerable attention in the fields of catalysis, surface science, and materials science, since polyoxometalates are often considered as molecular analogues of oxides in terms of structural analogy.[1,2] In fact, various types of titanium(IV)-containing polyoxometalates have been synthesized and structurally characterized because the multicentered titanium(IV) sites formed with the corner- and edge-sharing TiO_6 octahedra are expected to be used as the molecular models of titanium(IV)-containing solid materials. For example, the following have been reported: monomeric *mono*- and 1,5-*di*titanium(IV)-substituted Keggin polyoxotungstates $[\alpha\text{-}PTiW_{11}O_{40}]^{5-}$ and $[\alpha\text{-}1,5\text{-}PTi_2W_{10}O_{40}]^{7-}$;[3−7] dimeric *mono*titanium(IV)-substituted Keggin polyoxotungstate $[(\alpha\text{-}PTiW_{11}O_{39})_2OH]^{7-}$;[2] dimeric *di*titanium(IV)-substituted Keggin polyoxotungstates $[\alpha,\alpha\text{-}P_2W_{20}Ti_4O_{78}]^{10-}$ and $[\{\gamma\text{-}SiTi_2W_{10}O_{36}(OH)_2\}_2(\mu\text{-}O)_2]^{8-}$;[8,9] dimeric *tri*titanium(IV)-substituted Keggin polyoxotungstates [β,β-

* To whom correspondence should be addressed. E-mail: nomiya@chem.kanagawa-u.ac.jp.

(1) (a) Kholdeeva, O. A.; Trubisina, T. A.; Maksimovskaya, R. I.; Golovin, A. V.; Nelwert, W. A.; Kolesov, B. A.; López, X.; Poblet, J. M. *Inorg. Chem.* **2004**, *43*, 2284−2292. (b) Kholdeeva, O. A.; Trubitsina, T. A.; Maksimov, G. M.; Golovin, A. V.; Maksimovskaya, R. I. *Inorg. Chem.* **2005**, *44*, 1635−1642. (c) Kato, C. N.; Negishi, S.; Yoshida, K.; Hayashi, K.; Nomiya, K. *Appl. Catal., A: Gen.* **2005**, *292*, 97−104 and reference therein.

(2) Kholdeeva, O. A.; Maksimov, G. M.; Maksimovskaya, R. I.; Kovaleva, L. A.; Feditive, M. A.; Grigoviev, V. A.; Hill, C. L. *Inorg. Chem.* **2000**, *39*, 3828−3837.

(3) Kholdeeva, O. A.; Maksimov, G. M.; Maksimovskaya, R. I.; Kovaleva, L. A.; Fedotov, M. A. *React. Kinet. Catal. Lett.* **1999**, *66*, 311−317.

(4) Kholdeeva, O. A.; Maksimovskaya, R. I.; Maksimov, G. M.; Kovaleva, L. A. K*inet. Catal.* **2001**, *42*, 217−222.

(5) Yamase, T.; Ishikawa, E.; Asai, Y.; Kanai, S. *J. Mol. Catal., A: Chem.* **1996**, *114*, 237−245.

(6) Ishikawa, E.; Yamase, T. *J. Mol. Catal., A: Chem.* **1999**, *142*, 61−76.

(7) Gao, F.; Yamase, T.; Suzuki, H. *J. Mol. Catal., A: Chem.* **2002**, *180*, 97−108.

(8) Nomiya, K.; Takahashi, M.; Widegren, J. A.; Aizawa, T.; Sakai, Y.; Kasuga, N. C. *J. Chem. Soc., Dalton Trans.* **2002**, 3679−3685.

(9) Goto, Y.; Kamata, K.; Yamaguchi, K.; Uehara, K.; Hikichi, S.; Mizuno, N. *Inorg. Chem.* **2006**, *45*, 2347−2356.

10.1021/ic060656e CCC: $33.50 © 2006 American Chemical Society
Published on Web 09/02/2006

$Si_2W_{18}Ti_6O_{77}]^{14-}$,[10] [α,α-$Ge_2W_{18}Ti_6O_{77}]^{14-}$,[11] and [α,α-$P_2W_{18}Ti_6O_{77}]^{12-}$;[12] tetrameric anhydride forms of tetrapod-shaped *tri*titanium(IV)-substituted Dawson polyoxotungstates $[(P_2W_{15}Ti_3O_{57.5}(OH)_3)_4]^{24-}$,[13] $[(P_2W_{15}Ti_3O_{60.5})_4Cl]^{34-}$,[14] and $[(\alpha\text{-}1,2,3\text{-}P_2W_{15}Ti_3O_{62})_4\{\mu_3\text{-}Ti(OH)_3\}_4Cl]^{45-}$.[15]

Following the development of titanium(IV)-containing polyoxometalates, there has been a dramatic advance in recent years in the studies on various types of zirconium(IV) complexes with polyoxometalates. The reported crystal structures include a zirconocene complex $[(PW_{11}NbO_{40})_2ZrCp]^{6-}$,[16] the dimeric $[\{ZrW_5O_{18}(\mu\text{-}OH)\}_2]^{6-}$ anion[17] sandwich complexes containing 6-coordinate zirconium ions corresponding to the formulas $[Zr_3(\mu_2\text{-}OH)_3(A\text{-}\beta\text{-}SiW_9O_{34})_2]^{11-}$,[18] $[Zr_6O_2(OH)_4(H_2O)_3(\beta\text{-}SiW_{10}O_{37})_3]^{14-}$, and $[Zr_4O_2(OH)_2(H_2O)_4(\beta\text{-}SiW_{10}O_{37})_2]^{10-}$,[19] a mixed 6- and 7-coordinate zirconium complex $[Zr_2(\mu\text{-}OH)(H_2O)_2(AsOH)_2(AsW_7O_{28})(AsW_{10}O_{36})]^{9-}$,[20] a 7-coordinate zirconium ion $[Zr_4(\mu_3\text{-}O)_2(\mu_2\text{-}OH)_2(H_2O)_4(P_2W_{16}O_{59})_2]^{14-}$,[21] 8-coordinate zirconium complexes $[Zr(PMo_{12}O_{40})(PMo_{11}O_{39})]^{6-}$ [22] and $[(\alpha\text{-}P_2W_{16}O_{59})Zr_2(\mu_3\text{-}O)(malate)]_2^{18-}$,[23] and chiral zirconium ions $[\{\alpha\text{-}P_2W_{15}O_{55}(H_2O)\}Zr_3(\mu_3\text{-}O)(H_2O)(L\text{-}tartH)(\alpha\text{-}P_2W_{16}O_{59})]^{15-}$ and $[\{\alpha\text{-}P_2W_{15}O_{55}(H_2O)\}Zr_3(\mu_3\text{-}O)(H_2O)(D\text{-}tartH)(\alpha\text{-}P_2W_{16}O_{59})]^{15-}$.[24] However, examples of structurally characterized zirconium(IV) complexes with polyoxometalates are still rare, and hafnium(IV)-containing polyoxometalates have never been reported.

In this study, we successfully obtained a series of zirconium(IV) and hafnium(IV) complexes with Dawson and Keggin monovacant phosphotungstates in the form of crystals suitable for X-ray structure analyses of $K_{15}H[Zr(\alpha_2\text{-}P_2W_{17}O_{61})_2]\cdot 25H_2O$ (K-**1**), $K_{16}[Hf(\alpha_2\text{-}P_2W_{17}O_{61})_2]\cdot 19H_2O$ (K-**2**), $(Et_2NH_2)_{10}[Zr(\alpha\text{-}PW_{11}O_{39})_2]\cdot 7H_2O$ (Et_2NH_2-**3**), and $(Et_2NH_2)_{10}[Hf(\alpha\text{-}PW_{11}O_{39})_2]\cdot 2H_2O$ (Et_2NH_2-**4**). In this paper, we reported the complete details of the syntheses, characterization, and molecular structures of complexes **1**−**4**. Systematic studies on the influence of the lacunary polyoxoanion ligands on the nature of the bonding modes (bond lengths and bond angles) around the same coordination environment were also investigated.

Experimental Section

Materials and Methods. $K_{10}[\alpha_2\text{-}P_2W_{17}O_{61}]\cdot 19H_2O$ and $Na_3[\alpha\text{-}PW_{12}O_{40}]\cdot 11H_2O$ were prepared as described in the literature.[25,26] The number of solvated water molecules was determined by TG/DTA analyses. All reagents and solvents (methanol, ethanol, diethyl ether, and acetone) were obtained and used as received from commercial sources. Elemental analyses were carried out by Mikroanalytisches Labor Pascher (Remagen, Germany). The samples were dried overnight at room temperature under 10^{-3} to 10^{-4} Torr before analysis. Infrared spectra were recorded on a Jasco 300 FT-IR spectrometer in KBr disks at room temperature. Thermogravimetric (TG) and differential thermal analyses (DTA) were acquired using a Rigaku TG8101D and TAS 300 data-processing system. TG/DTA measurements were run under air with a temperature ramp of 4 °C/min between 20 and 500 °C. ^{31}P NMR (161.70 MHz) spectra in D_2O solution were recorded in 5-mm outer diameter tubes on a JEOL JNM-EX 400 FT-NMR spectrometer and a JEOL EX-400 NMR data-processing system. ^{31}P NMR spectra were referenced to an external standard of 25% H_3PO_4 in H_2O in a sealed capillary. Chemical shifts were reported as negative on the δ scale for resonances upfield of H_3PO_4 (δ 0). ^{31}P NMR signals were shifted to −0.101 ppm by using 85% H_3PO_4 as a reference instead of 25% H_3PO_4. ^{183}W NMR (16.50 MHz) spectra were recorded in 10-mm outer diameter tubes on a JEOL JNM-EX 400 FT-NMR spectrometer equipped with a JEOL NM-40T10L low-frequency tunable probe and a JEOL EX-400 NMR data-processing system. ^{183}W NMR spectra measured in D_2O were referenced to an external standard of saturated Na_2WO_4−D_2O solution (substitution method). Chemical shifts were reported as negative for resonances upfield of Na_2WO_4 (δ 0). ^{183}W NMR signals were shifted to −0.787 ppm by using 2 M Na_2WO_4 solution as a reference instead of saturated Na_2WO_4 solution.

Synthesis of $K_{15}H[Zr(\alpha_2\text{-}P_2W_{17}O_{61})_2]\cdot 25H_2O$ (K-1) and $K_{16}[Hf(\alpha_2\text{-}P_2W_{17}O_{61})_2]\cdot 19H_2O$ (K-2). $ZrCl_2O\cdot 8H_2O$ (0.40 g, 1.24 mmol) or $HfCl_2O\cdot 8H_2O$ (0.38 g, 0.93 mmol) was dissolved in 60 mL of water and the solution stirred for 5 min in a water bath at 90 °C. To the vigorously stirred, clear, colorless solution, 6.14 g (1.24 mmol) of solid $K_{10}[\alpha_2\text{-}P_2W_{17}O_{61}]\cdot 19H_2O$ was added instantly. This solution was stirred for 30 min and then cooled to room temperature. The colorless solution was filtered through a folded filter paper (Whatman No. 4). The colorless filtrate was added to vigorously stirred methanol (300 mL) at room temperature. After the solution was stirred for 1 h, a white precipitate was formed in the methanol; this precipitate was collected on a membrane filter (JG 0.2 μm) and washed with methanol (50 mL × 3) and ether (50 mL × 3). At this stage, the crude product of the potassium salt was obtained in 5.54 and 5.48 g yield, respectively. This crude product (1.0 g) was dissolved in 2.5 mL of water for **1** and 2.0 mL of water for **2** by stirring in a water bath at 90 °C. The colorless

(10) Lin, Y.; Weakley, T. J. R.; Rapko, B.; Finke, R. G. *Inorg. Chem.* **1993**, *32*, 5095−5101.
(11) Yamase, T.; Ozeki, T.; Sakamoto, H.; Nishiya, S.; Yamamoto, A. *Bull. Chem. Soc. Jpn.* **1993**, *66*, 103−108.
(12) Nomiya, K.; Takahashi, M.; Ohsawa, K.; Widegren, J. A. *J. Chem. Soc., Dalton Trans.* **2001**, 2872−2878.
(13) Kortz, U.; Hamzeh, S. S.; Nasser, N. A. *Chem.—Eur. J.* **2003**, *9*, 2945−2952.
(14) Sakai, Y.; Yoza, K.; Kato, C. N.; Nomiya, K. *Dalton Trans.* **2003**, 3581−3586.
(15) Sakai, Y.; Yoza, K.; Kato, C. N.; Nomiya, K. *Chem.—Eur. J.* **2003**, *9*, 4077−4083.
(16) Radkov, E. V.; Young. V. G., Jr.; Beer, R. H. *J. Am. Chem. Soc.* **1999**, *121*, 8953−8954.
(17) Villanneau, R.; Carabineiro, H.; Carrier, X.; Thouvenot, R.; Herson, P.; Lemos, F.; Ribeiro, F. R.; Che, M. *J. Phys. Chem. B* **2004**, *108*, 12465−12471.
(18) Finke, R. G.; Rapko, B.; Weakley, T. J. R. *Inorg. Chem.* **1989**, *28*, 1573−1579.
(19) Bassil, B. S.; Dickman, M. H.; Kortz, U. *Inorg. Chem.* **2006**, *45*, 2394−2396.
(20) Gaunt, A. J.; May, I.; Collison, D.; Helliwell, M. *Acta Crystallogr.* **2003**, *C59*, i65−i66.
(21) Gaunt, A. J.; May, I.; Collison, D.; Holman, K. T.; Pope, M. T. *J. Mol. Struct.* **2003**, *656*, 101−106.
(22) Gaunt, A. J.; May, I.; Collison, D.; Fox, O. D. *Inorg. Chem.* **2003**, *42*, 5049−5051.
(23) Fang, X.; Anderson, T. M.; Hou, Y.; Hill, C. L. *Chem. Commun.* **2005**, 5044−5046.
(24) Fang, X.; Anderson, T. M.; Hill, C. L. *Angew. Chem., Int. Ed.* **2005**, *44*, 3540−3544.
(25) Lyon, D. K.; Miller, W. K.; Novet, T.; Domaille, P. J.; Evitt, E.; Johnson, D. C.; Finke, R. G. *J. Am. Chem. Soc.* **1991**, *113*, 7209−7221.
(26) Rosenheim, A.; Jaenicke, J. *Z. Anorg. Allg. Chem.* **1917**, *101*, 235−275.

solution was then allowed to evaporate slowly at room temperature. After 1 day, clear colorless granular crystals were formed. The crystals were obtained in 64.0% yield (0.67 g scale) based on $K_{15}H[Zr(\alpha_2\text{-}P_2W_{17}O_{61})_2]\cdot 25H_2O$ and 39.2% yield (0.42 g scale) based on $K_{16}[Hf(\alpha_2\text{-}P_2W_{17}O_{61})_2]\cdot 19H_2O$. Compounds K-**1** and K-**2** were soluble in water but insoluble in diethyl ether and methanol. Characterization results for K-**1**: Anal. Found: H, 0.34; K, 6.43; P, 1.36; W, 68.4; Zr, 1.27; O, 21.8; Cl, <0.02%; total 99.6%. Calcd for $K_{15}H[Zr(\alpha_2\text{-}P_2W_{17}O_{61})_2]\cdot 6H_2O = H_{13}K_{15}P_4W_{34}Zr_1O_{128}$: H, 0.14; K, 6.44; P, 1.36; W, 68.59; Zr, 1.00; O, 22.47. A weight loss of 3.4% was observed during the course of drying at room temperature at $10^{-3}-10^{-4}$ Torr overnight before analysis, suggesting the presence of 18−19 weakly solvated or adsorbed water molecules. TG/DTA under atmospheric conditions: a weight loss of 4.78% was observed below 500 °C with an endothermic peak at 86.0 °C; calcd 4.76% for $y = 25$ in $K_{15}H[Zr(\alpha_2\text{-}P_2W_{17}O_{61})_2]\cdot yH_2O$. IR (KBr disk): 1085 s, 1060 m, 1035 m, 1017 m, 944 s, 924 s, 803 s, 738 s, 605 w, 567 w, 526 m cm^{-1}. ^{31}P NMR (22.8 °C, D_2O): δ −9.20, −13.81. ^{183}W NMR (23.7 °C, D_2O): δ −128.0 (1 + 1W), −167.0 (1W), −172.1 (1W), −176.3 (1W), −184.1 (1W), −186.2 (1W), −199.9 (1W), −202.4 (1W), −205.0 (1W), −207.4 (1W), −208.5 (1W), −209.7 (1W), −214.6 (1W), −228.6 (1W), −236.2 (1W), −252.1 (1W). Characterization results for K-**2**: Anal. Found: H, 0.18; K, 6.74; P, 1.30; W, 67.6; Hf, 2.21. Calcd for $K_{16}[Hf(\alpha_2\text{-}P_2W_{17}O_{61})_2]\cdot 9H_2O = H_{18}K_{16}P_4W_{34}Hf_1O_{131}$: H, 0.20; K, 6.73; P, 1.33; W, 67.27; Hf, 1.92. A weight loss of 1.86% was observed during the course of drying at room temperature at $10^{-3}-10^{-4}$ Torr overnight before analysis, suggesting the presence of 9−10 weakly solvated or adsorbed water molecules. TG/DTA under atmospheric conditions: a weight loss of 3.59% was observed below 500 °C with an endothermic peak at 67.5 °C; calcd 3.61% for $y = 19$ in $K_{16}[Hf(\alpha_2\text{-}P_2W_{17}O_{61})_2]\cdot yH_2O$. IR (KBr disk): 1085 s, 1060 m, 1037 m, 1016 m, 944 s, 922 s, 811 s, 745 s, 605 w, 570 w, 526 m cm^{-1}. ^{31}P NMR (23.6 °C, D_2O): δ −9.25, −13.82. ^{183}W NMR (22.2 °C, D_2O): δ −127.2 (1 + 1W), −162.1 (1W), −166.3 (1W), −176.0 (1W), −184.3 (1W), −186.2 (1W), −199.5 (1W), −202.0 (1W), −204.3 (1W), −206.7 (1W), −207.5 (1W), −208.8 (1W), −211.1 (1W), −229.2 (1W), −237.1 (1W), −247.7 (1W).

Synthesis of $(Et_2NH_2)_{10}[Zr(PW_{11}O_{39})_2]\cdot 7H_2O$ (Et_2NH_2-3) and $(Et_2NH_2)_{10}[Hf(\alpha\text{-}PW_{11}O_{39})_2]\cdot 2H_2O$ (Et_2NH_2-4). $Na_3[\alpha\text{-}PW_{12}O_{40}]\cdot 11H_2O$ (5.0 g, 1.59 mmol) was dissolved in 50 mL of water. Na_2CO_3 (0.355 g, 3.35 mmol) was added slowly to the colorless solution and stirred for 20 min. The pH of this solution was estimated to be 4.0 at this stage. $ZrCl_2O\cdot 8H_2O$ (0.256 g, 0.79 mmol) or $HfCl_2O\cdot 8H_2O$ (0.326 g, 0.79 mmol) was added to the solution instantly and stirred for 5 min at 25 °C. To the vigorously stirred, clear, colorless solution, 1 mL of 1 M HCl(aq) was added for 1 min. The clear colorless solution was stirred for 30 min at 25 °C. This solution was filtered through a folded filter paper (Whatman No. 4). The colorless filtrate was evaporated to ca. 15 mL at 40 °C and then cooled to room temperature. Et_2NH_2Cl (2.5 g, 22.8 mmol) was added and stirred for 1 h. A white precipitate was formed and collected on a membrane filter (JG 0.2 μm); the precipitate was then washed with ethanol (50 mL × 3) and ether (50 mL × 3). At this stage, the crude product of the diethylammonium salt was obtained in 4.20 and 4.46 g yield, respectively. This crude product (4.20 g for **3** and 4.46 g for **4**) was suspended in 15 mL of water. After being stirred for 1 h, the suspension was filtered through a folded filter paper (Whatman No. 2), following which the filtrate was added to acetone (500 mL). After the solution was stirred for 1 h, a white precipitate was formed and collected on a membrane filter (JG 0.2 μm); this precipitate was washed with acetone (30 mL × 3) and ether (50 mL × 3). The resultant product (2.57 g for **3** and 3.28 g for **4**) was dissolved in 15 mL of water at 25 °C. The colorless filtrate was evaporated to ca. 7 mL at 40 °C and then filtered through a folded filter paper (Whatman No. 2). The colorless solution was then allowed to evaporate slowly at room temperature. After 1 day, clear colorless needle crystals for Et_2NH_2-**3** and clear colorless prism crystals for Et_2NH_2-**4** were formed. The crystals were collected on a membrane filter (JG 0.2 μm) and washed with ethanol (30 mL × 3) and ether (50 mL × 3). The crystals were obtained in 10.2% yield (0.51 g scale) based on $(Et_2NH_2)_{10}[Zr(\alpha\text{-}PW_{11}O_{39})_2]\cdot 7H_2O$ and 11.8% yield (0.59 g scale) based on $(Et_2NH_2)_{10}[Hf(\alpha\text{-}PW_{11}O_{39})_2]\cdot 2H_2O$. Compounds Et_2NH_2-**3** and Et_2NH_2-**4** were soluble in water but insoluble in diethyl ether, ethanol, and acetone. Characterization results for Et_2NH_2-**3**: Anal. Found: H, 2.07; C, 7.40; N, 2.31; P, 0.95; W, 65.5; Zr, 1.45. Calcd for $(Et_2NH_2)_{10}[Zr(\alpha\text{-}PW_{11}O_{39})_2]\cdot 3H_2O = C_{40}H_{126}N_{10}P_2W_{22}Zr_1O_{81}$: H, 2.03; C, 7.70; N, 2.24; P, 0.99; W, 64.81; Zr, 1.46. A weight loss of 1.23% was observed during the course of drying at room temperature at $10^{-3}-10^{-4}$ Torr overnight before analysis, suggesting the presence of 4−5 weakly solvated or adsorbed water molecules. TG/DTA under atmospheric conditions: a weight loss of 1.94% was observed below 148 °C; calcd 2.00% for $y = 7$ in $(Et_2NH_2)_{10}[Zr(\alpha\text{-}PW_{11}O_{39})_2]\cdot yH_2O$. A weight loss of 11.91% with an endothermic peak at 266.0 °C, and an exothermic peak at 375.0 °C was observed in the temperature range of 148−500 °C, which would be due to the decomposition of $Et_2NH_2^+$ ions (calcd value for 10 $Et_2NH_2^+$ ions was 11.71%). IR (KBr disk): 1473 m, 1458 m, 1390 m, 1197 w, 1159 w, 1120 s, 1054 s, 954 s, 884 s, 823 s, 745 s, 600 w, 516 m, 487 w, 436 w cm^{-1}. ^{31}P NMR (22.8 °C, D_2O): δ −14.57, −14.65. Characterization results for Et_2NH_2-**4**: Anal. Found: H, 2.01; C, 7.61; N, 2.23; P, 0.93; W, 64.8; Hf, 2.82. Calcd for $(Et_2NH_2)_{10}[Hf(\alpha\text{-}PW_{11}O_{39})_2] = C_{40}H_{120}N_{10}P_2W_{22}Hf_1O_{78}$: H, 1.93; C, 7.66; N, 2.23; P, 0.99; W, 64.46; Hf, 2.84. A weight loss of 0.63% was observed during the course of drying at room temperature at $10^{-3}-10^{-4}$ Torr overnight before analysis, suggesting the presence of 2−3 weakly solvated or adsorbed water molecules. TG/DTA under atmospheric conditions: a weight loss of 0.35% was observed below 180 °C; calcd 0.57% for $y = 2$ in $(Et_2NH_2)_{10}[Hf(\alpha\text{-}PW_{11}O_{39})_2]\cdot yH_2O$. A weight loss of 11.87% was observed with endothermic peaks at 53.5 and 266.3 °C and an exothermic peak at 374.5 °C was observed in the temperature range of 180−500 °C, which would be due to the decomposition of $Et_2NH_2^+$ ions (calcd value for 10 $Et_2NH_2^+$ ions was 11.68%). IR (KBr disk): 1472 m, 1455 m, 1392 m, 1308 m, 1197 w, 1159 w, 1121 s, 1055 s, 955 s, 887 s, 825 s, 749 s, 600 w, 514 m, 485 w cm^{-1}. ^{31}P NMR (16.7 °C, D_2O): δ −14.67, −14.77.

X-ray Crystallography. Crystals of complexes **1**−**4** were surrounded by liquid paraffin to prevent their degradation. Data collection was carried out by Bruker SMART APEX CCD diffractometer at 90 K. The intensity data were automatically corrected for Lorentz and polarization effects during integration. The structure was solved by direct methods (SHELXS-97; Sheldrick, 1990),[27] followed by subsequent difference Fourier calculation, and refined by the full-matrix least-squares procedures (SHELXL-97; Sheldrick, 1997).[28] Absorption correction was performed with

(27) Sheldrick, G. M. *Acta Crystallogr., Sect. A* **1990**, *46*, 467−473.
(28) Sheldrick, G. M. *SHELXL-97 program for crystal structure refinement*; University of Goettingen: Goettingen, Germany, 1997.

SADABS (empirical absorption correction).[29] For complexes **1** and **2**, 34 tungsten atoms, 1 atom each of zirconium and hafnium, and 4 phosphorus atoms were clearly identified. For complexes **3** and **4**, 22 tungsten atoms, 1 atom each of zirconium and hafnium, and 2 phosphorus atoms were clearly identified. Thus, the main features of the molecular structures of the polyoxometalates were clarified. However, the resolution obtained for the structure of the salt was limited by the poor quality of the available crystals and by the considerable disorder of the countercations and the solvent of crystallization. These features are common in polyoxometalate crystallography.[12,30] Further details on the crystal structure investigation may be obtained from the Fachinformationzentrum Karlsruhe, 76344 Eggenstein-Leopoldshafen, Germany (fax, (+49) 7247-808-666); e-mail, crysdata@fiz-karlsruhe.de), on quoting the depository nos. CSD-416348, CSD-416349, CSD-416346, and CSD-416347 for complexes **1**−**4**, respectively.

Results and Discussion

Syntheses, Characterization, and Molecular Structures of the Zirconium(IV) and Hafnium(IV) Complexes with $[\alpha_2\text{-}P_2W_{17}O_{61}]^{10-}$ (Complexes 1 and 2). The zirconium and hafnium complexes containing $[\alpha_2\text{-}P_2W_{17}O_{61}]^{10-}$, both compounds **1** and **2** with C_2 symmetry, were obtained in 64.0% and 39.2% yields, respectively, based on the potassium salts, $K_{15}H[Zr(\alpha_2\text{-}P_2W_{17}O_{61})_2]\cdot 25H_2O$ (K-**1**) and $K_{16}[Hf(\alpha_2\text{-}P_2W_{17}O_{61})_2]\cdot 19H_2O$ (K-**2**). Compounds K-**1** and K-**2** were prepared by the ratio of 1:1 and 0.75:1 reactions of $K_{10}[\alpha_2\text{-}P_2W_{17}O_{61}]\cdot 21H_2O$ with $ZrCl_2O\cdot 8H_2O$ and $HfCl_2O\cdot 8H_2O$, respectively, in an aqueous solution (when $K_{10}[\alpha_2\text{-}P_2W_{17}O_{61}]\cdot 21H_2O$ was added to the aqueous solutions of $ZrCl_2O\cdot 8H_2O$ and $HfCl_2O\cdot 8H_2O$, the pH changed from 2.2 to 6.6), followed by reprecipitation from water/methanol and crystallization from hot water (>90 °C). The unreacted zirconium and hafnium species were completely removed from water by crystallization. It was noted that the analytically pure complexes **1** and **2** were not obtained by the 2:1 ratio reaction of $[\alpha_2\text{-}P_2W_{17}O_{61}]^{10-}$ with MCl_2O (M = Zr, Hf) even when the pH of the solution was adjusted to 4.5 by 1 M HCl(aq) because of the formation of $[\alpha\text{-}P_2W_{18}O_{62}]^{6-}$. The formation of **1** and **2** can be shown in an ionic balanced equation:

$$2[\alpha_2\text{-}P_2W_{17}O_{61}]^{10-} + MCl_2O + 2H^+ \rightarrow [M(\alpha_2\text{-}P_2W_{17}O_{61})_2]^{16-}\ (M = Zr, Hf) + 2Cl^- + H_2O \quad (1)$$

The molecular structures of the anions **1** and **2** shown in Figure 1a,b demonstrated that the Zr(IV) and Hf(IV) ions were coordinated to two monovacant sites in the "cap" regions of two $[\alpha_2\text{-}P_2W_{17}O_{61}]^{10-}$; these structures were identical with that of the reported $[Lu(\alpha_2\text{-}P_2W_{17}O_{61})_2]^{17-}$.[31] The two polyoxometalate "lobes" are oriented in a *syn* fashion. The crystal data for K-**1** and K-**2** are summarized in Table 1. The polyoxoanions **1** and **2** were detected as a set of an enantiomeric pair of units in the unit cell. The Zr(IV) and Hf(IV) ions are located in a square antiprismatic coordination environment with eight oxygen atoms, four of them being provided from each of the two $[\alpha_2\text{-}P_2W_{17}O_{61}]^{10-}$ ligands, as shown in Figure 2a. The Zr−O and Hf−O bond lengths were in the ranges 2.172−2.229 Å (average 2.203 Å) and 2.158−2.219 Å (2.186 Å), respectively (Table S1, Supporting Information). The Zr−O bond length was reproduced two times by X-ray crystallography for complex **1** (the difference of the average Zr−O bond length between the first and the second analysis was 0.005 Å). The Zr−O and Hf−O bond lengths are shorter than those of the Dawson-type lanthanide and actinide atom-coordinated polyoxotungstates $[X(\alpha_2\text{-}P_2W_{17}O_{61})_2]^{16-/17-}$ (X = Lu^{3+}, Pu^{4+}, Np^{4+}, Th^{4+}, Eu^{3+}, Am^{3+}, Sm^{3+}, Pu^{3+}, Np^{3+}, and Ce^{3+}; 2.31−2.52 Å), and the bond length increased with an increase in the ionic radii of the coordinated atoms.[31−33] The tungsten−oxygen and phosphorus−oxygen bond lengths and angles of the two polyoxoanion ligands for K-**1** and K-**2** are consistent with those of $[Lu(\alpha_2\text{-}P_2W_{17}O_{61})_2]^{17-}$, as shown in Tables S2 and S3. The values of the bond valence sums (BVS) for K-**1**,[34] which were calculated on the basis of the observed bond lengths, were 3.812 for the Zr(1) atom and in the range 6.030−6.219 for the 34 W atoms, 4.896−4.921 for the two P atoms, and 1.609−2.123 for the 122 O atoms; these values reasonably corresponded to the formal valences of Zr^{4+}, W^{6+}, P^{5+}, and O^{2-}, respectively (Table S4). The BVS values for K-**2** were 4.164 for the Hf(1) atom, in the range 5.939−6.314 for the 34 W atoms, 4.872−4.908 for the two P atoms, and 1.609−2.103 for the 122 O atoms; these values also reasonably corresponded to the formal valences of Hf^{4+}, W^{6+}, P^{5+}, and O^{2-}, respectively (Table S5).

The crystal structures of complexes **1** and **2** were consistent with the elemental analyses, TG/DTA, FTIR, and ^{31}P and ^{183}W NMR spectroscopy. The elemental analyses performed for K-**1** and K-**2**, dried at room temperature at 10^{-3}−10^{-4} Torr overnight, were consistent with a composition of $K_{15}H[Zr(\alpha_2\text{-}P_2W_{17}O_{61})_2]\cdot 6H_2O$ and $K_{16}[Hf(\alpha_2\text{-}P_2W_{17}O_{61})_2]\cdot 9H_2O$, respectively. The weight loss observed during the course of drying before analysis was 3.4% for K-**1** and 1.86% for K-**2**; this corresponded to 19 and 10 weakly solvated or adsorbed water molecules for K-**1** and K-**2**, respectively. TG/DTA

(29) Sheldrick, G. M. *SADABS*; University of Goettingen: Goettingen, Germany, 1996.

(30) (a) Weakley, T. J. R.; Finke, R. G. *Inorg. Chem.* **1990**, *29*, 1235−1241. (b) Lin, Y.; Weakley, T. J. R.; Rapko, B.; Finke, R. G. *Inorg. Chem.* **1993**, *32*, 5095−5101. (c) Yamase, T.; Ozeki, T.; Sakamoto, H.; Nishiya, S.; Yamamoto, A. *Bull. Chem. Soc. Jpn.* **1993**, *66*, 103−108. (d) Nomiya, K.; Takahashi, M.; Widegren, J. A.; Aizawa, T.; Sakai, Y.; Kasuga, N. C. *J. Chem. Soc., Dalton Trans.* **2002**, 3679−3685.

(31) Luo, Q.-H.; Howell, R. C.; Dankova, M.; Bartis, J.; Williams, C. W.; Horrocks, W. D., Jr.; Young, V. G., Jr.; Rheingold, A. L.; Francesconi, L. C.; Antonio, M. R. *Inorg. Chem.* **2001**, *40*, 1894−1901.

(32) Antonio, M. R.; Soderholm, L.; Williams, C. W.; Ullah, N.; Francesconi, L. C. *J. Chem. Soc., Dalton Trans.* **1999**, 3825−3830.

(33) Chiang, M.-H.; Williams, C. W.; Soderholm, L.; Antonio, M. R. *Eur. J. Inorg. Chem.* **2003**, 2663−2669.

(34) (a) Brown, I. D.; Altermatt, D. *Acta Crystallogr., Sect. B* **1985**, *B41*, 244−247. (b) Brown, I. D.; Shannon, R. D. *Acta Crystallogr. Sect. A* **1973**, *A29*, 266−282. (c) Brown, I. D. *Acta Crystallogr. Sect. B* **1992**, *B48*, 553−572. (d) Brown, I. D. J. *App. Crystallogr.* **1996**, *29*, 479−480.

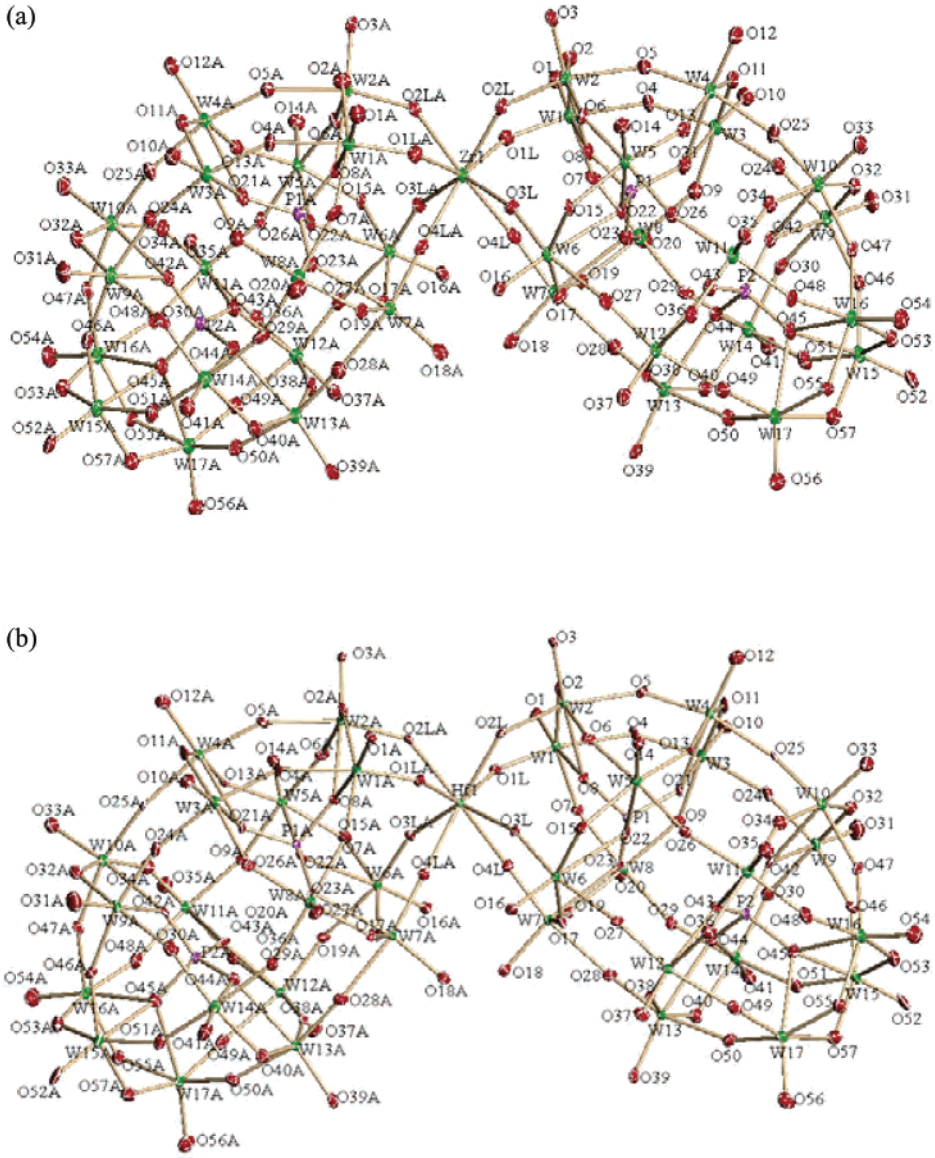

Figure 1. Molecular structures of (a) $[Zr(\alpha_2\text{-}P_2W_{17}O_{61})_2]^{16-}$ (**1**) and (b) $[Hf(\alpha_2\text{-}P_2W_{17}O_{61})_2]^{16-}$ (**2**) with 50% probability ellipsoids.

measurements performed under atmospheric conditions showed a weight loss of 4.78% and 3.59% for K-**1** and K-**2** with endothermic peaks at 86.0 and 67.5 °C, respectively; this corresponded to the presence of 25 and 19 water molecules due to both intrinsic water of hydration and adsorbed water from the atmosphere. Thus, the number of hydrated water molecules in compounds **1** and **2** are described as 25 and 19, respectively.

The FTIR spectra of K-**1** and K-**2**, which were measured as KBr disks, showed the characteristic vibrational bands of the Dawson-type "$P_2W_{18}O_{62}^{6-}$" polyoxotungstate framework (Figure S1a,b).[35] The positions of all the bands in the polyoxoanion region in **1** and **2** were very similar to those of the $[\alpha_2\text{-}P_2W_{17}O_{61}]^{10-}$ (Figure S1c; 1086 s, 1054 m, 1016 m, 940 s, 885 s, 811 s, 741 s, 601 m, 527 w, 467 w cm^{-1}), indicating that the structure of $[\alpha_2\text{-}P_2W_{17}O_{61}]^{10-}$ was retained after the coordination of Zr and Hf atoms onto the monovacant site of the $[\alpha_2\text{-}P_2W_{17}O_{61}]^{10-}$ ligand.

The ^{31}P NMR spectra of **1** and **2** in D_2O at 25 °C showed a clean two-line spectrum at −9.20 and −13.81 ppm and −9.25 and −13.82 ppm, respectively, thereby confirming its purity and homogeneity (Figure 3a,b). The downfield resonance is assigned to the phosphorus closest to the Zr and Hf sites, whereas the upfield resonance is due to the phosphorus closer to the W_3 cap. These signals exhibited a shift from that of $[\alpha_2\text{-}P_2W_{17}O_{61}]^{10-}$ (Figure 3c; −6.96 and −14.10 ppm), thereby showing the coordination of Zr and Hf atoms onto the monovacant site of $[\alpha_2\text{-}P_2W_{17}O_{61}]^{10-}$ ligand. The ^{183}W NMR spectra (Figure 4a,b) of **1** and **2** measured in D_2O at 23.7 and 22.2 °C, respectively, showed 17-line spectra of δ −128.0 (1 + 1W), −167.0 (1W), −172.1 (1W), −176.3 (1W), −184.1 (1W), −186.2 (1W), −199.9 (1W), −202.4 (1W), −205.0 (1W), −207.4 (1W), −208.5 (1W), −209.7 (1W), −214.6 (1W), −228.6 (1W), −236.2

(35) Rocciccioli-Deltcheff, C.; Thouvenot, R. *Spectrosc. Lett.* **1979**, *12*, 127−138.

Table 1. Crystal Data for Compounds K-**1** and K-**2**

param	K-**1**	K-**2**
empirical formula	$H_{51}K_{15}O_{147}P_4W_{34}Zr$	$H_{38}HfK_{16}O_{141}P_4W_{34}$
fw	9455.91	9473.17
temp (K)	90(2)	90(2)
wavelength (Å)	0.710 73	0.710 73
cryst system	monoclinic	monoclinic
space group	*C*2/*c*	*C*2/*c*
unit cell dimens (Å, deg)	$a = 47.374(5)$	$a = 47.313(16)$
	$b = 14.4975(15)$	$b = 14.546(5)$
	$c = 22.739(2)$	$c = 22.827(8)$
	$\alpha = 90$	$\alpha = 90$
	$\beta = 91.1410(10)$	$\beta = 91.163(7)$
	$\gamma = 90$	$\gamma = 90$
V (Å^3)	15 614(3)	15 707(9)
Z	4	4
D(calcd) (Mg/m^3)	4.023	4.006
abs coeff (mm^{-1})	25.543	26.008
F(000)	16 512	16 472
cryst size (mm^3)	0.46 × 0.23 × 0.15	0.09 × 0.03 × 0.01
θ range for data collcn (deg)	0.86−28.34	0.86−28.45
index ranges	$-61 \le h \le 62, -19 \le k \le 19, -29 \le l \le 29$	$-62 \le h \le 63, -19 \le k \le 19, -30 \le l \le 30$
reflcns collcd	112 055	89 735
indpndt reflcns	19 021 [R(int) = 0.0661]	19 528 [R(int) = 0.0926]
refinement method	full-matrix least squares on F^2	full-matrix least squares on F^2
data/restraints/params	19 021/0/969	19 528/612/915
GOF on F^2	1.088	1.062
final R indices [$I > 2\sigma(I)$]	R1 = 0.0458, wR2 = 0.1281	R1 = 0.0583, wR2 = 0.1371
R indices (all data)	R1 = 0.0509, wR2 = 0.1330	R1 = 0.0879, wR2 = 0.1544
largest diff peak and hole (e•Å^{-3})	8.930 and −3.787	8.007 and −2.803

(1W), and −252.1 (1W) and δ −127.2 (1 + 1W), −162.1 (1W), −166.3 (1W), −176.0 (1W), −184.3 (1W), −186.2 (1W), −199.5 (1W), −202.0 (1W), −204.3 (1W), −206.7 (1W), −207.5 (1W), −208.8 (1W), −211.1 (1W), −229.2 (1W), −237.1 (1W), and −247.7 (1W). These values were different from those of $[\alpha_2\text{-}P_2W_{17}O_{61}]^{10-}$ (Figure 4c; δ −117.1 (2W), −140.4 (2W), −151.7 (2W), −181.0 (2W), −183.1 (1W), −218.1 (2W), −220.5 (2W), −224.0 (2W), and −242.6 (2W) with C_s symmetry). This indicates that the coordination of Zr and Hf atoms onto the monovacant site of $[\alpha_2\text{-}P_2W_{17}O_{61}]^{10-}$ ligand. The 17-line spectrum of K-**1** and K-**2** showed that the 17 tungsten atoms in each oxoanion half correspond to the other by a 2-fold rotation in solution. Thus, both Zr and Hf ions are coordinated to the α-Dawson polyoxoanion with C_2 symmetry. These ^{183}W and ^{31}P NMR spectra are consistent with the X-ray structures,

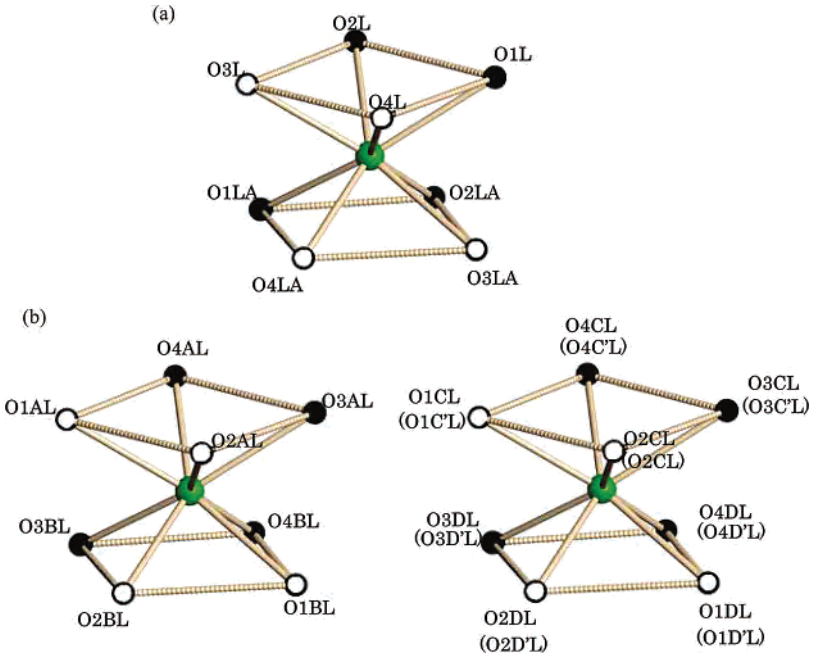

Figure 2. The coordination environments of Zr and Hf sites in (a) K-**1** and K-**2** and (b) Et_2NH_2-**3** and Et_2NH_2-**4**. The numbers in parentheses correspond to Et_2NH_2-**3**. The white, black, and green circles represent the terminal oxygen atoms bound to corner-sharing tungsten atoms, the terminal oxygen atoms bound to the edge-sharing tungsten atoms, and zirconium and hafnium center atoms, respectively.

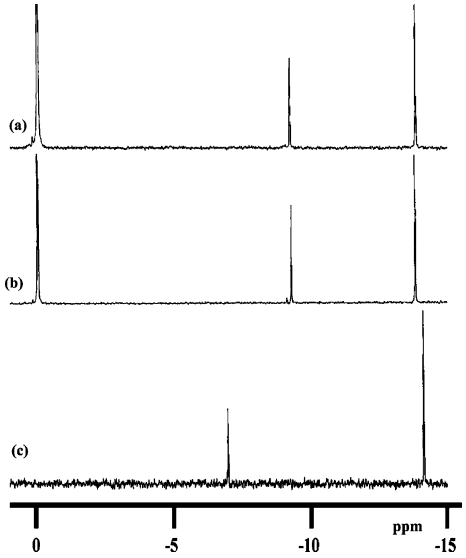

Figure 3. ^{31}P NMR spectra in D_2O of (a) K-**1**, (b) K-**2**, and (c) $[\alpha_2\text{-}P_2W_{17}O_{61}]^{10-}$.

suggesting that the solid structures are maintained in the solution.

Syntheses, Characterization, and Molecular Structures of the Zirconium(IV) and Hafnium(IV) Complexes with $[\alpha\text{-}PW_{11}O_{39}]^{7-}$ (Complexes 3 and 4). The zirconium and hafnium complexes contained in situ-generated $[\alpha\text{-}PW_{11}O_{39}]^{7-}$ by a reaction of $[\alpha\text{-}PW_{12}O_{40}]^{3-}$ with Na_2CO_3 in an aqueous solution; both compounds **3** and **4** with C_2 symmetry were obtained in 10.2% and 11.8% yields, respectively, based on the diethylammonium salts, $(Et_2NH_2)_{10}[Zr(\alpha\text{-}PW_{11}O_{39})_2]\cdot 7H_2O$ (Et_2NH_2-**3**) and $(Et_2NH_2)_{10}[Hf(\alpha\text{-}PW_{11}O_{39})_2]\cdot 2H_2O$ (Et_2NH_2-**4**). Compounds Et_2NH_2-**3** and Et_2NH_2-**4** were prepared by the ratio of 2:1 reactions of in situ-generated $[\alpha\text{-}PW_{11}O_{39}]^{7-}$ with $ZrCl_2O\cdot 8H_2O$ and $HfCl_2O\cdot 8H_2O$ in an aqueous solution, followed by the addition of 1 M HCl(aq) and excess amount of solid Et_2NH_2Cl. The obtained Et_2NH_2 salts of **3** and **4** were crystallized from water (40 °C). The formation of **3** and **4** can be shown in ionic balanced equations:

$$[\alpha\text{-}PW_{12}O_{40}]^{3-} + 2Na_2CO_3 + H_2O \rightarrow [\alpha\text{-}PW_{11}O_{39}]^{7-} + WO_4^{2-} + 2CO_2\uparrow + 4Na^+ + 2H^+ \quad (2)$$

$$2[\alpha\text{-}PW_{11}O_{39}]^{7-} + MCl_2O + 2H^+ \rightarrow [M(\alpha\text{-}PW_{11}O_{39})_2]^{17-} (M = Zr, Hf) + 2Cl^- + H_2O \quad (3)$$

The molecular structures of anions **3** and **4** are shown in Figures 5 and 6. In the crystallography, two different units (AB and CD) of anions **3** and **4** were observed. Both units of **3** and **4** showed a square antiprismatic coordination environment with eight oxygen atoms, four of them being provided from each of the two $[\alpha\text{-}PW_{11}O_{39}]^{7-}$ ligands with C_2 symmetry, similar to complexes **1** and **2** (Figure 2b). The crystal data for Et_2NH_2-**3** and Et_2NH_2-**4** are summarized in Table 2. The polyoxoanions **3** and **4** were detected as two sets of enantiomeric pairs of two different units in the unit cell. For comparison of the bonding modes between complexes **3** and **4**, the unit C′D′ was used for complex **3**. The Zr−O and Hf−O bond lengths were in the range 2.16−2.24 Å (average 2.21 Å) for Zr(1), 2.174−2.24 Å (2.21 Å) for Zr(2), 2.168−2.229 Å (2.199 Å) for Hf(1), and 2.157−2.227 Å (2.193 Å) for Hf(2) (Table S6). The Zr−O and Hf−O bond lengths are longer than those of complexes **1** and **2** and shorter than that of uranium(III)-coordinated polyoxotungstate $[U(GeW_{11}O_{39})_2]^{12-}$ (average 2.40 Å).[36] The tendency that the bond length of Zr−O was longer than that of Hf−O was observed for both Dawson and Keggin polyanions. The two polyoxometalate "lobes" are oriented in a *syn* fashion as well as complexes **1** and **2**. The tungsten−oxygen and phosphorus−oxygen bond lengths and angles of the two polyoxoanion ligands are consistent with the structure of $[\alpha\text{-}PW_{12}O_{40}]^{3-}$, as shown in Tables S7 and S8.[37] The BVS values for **3** were 3.793 for the Zr(1) atom and 3.773 for the Zr(2) atom. Further, these values were in the range 5.708−6.390 for the 22 W(1A−11B) atoms and 5.780−6.491 for the 22 W(1C′−11D′) atoms, 4.609−4.739 for the 2 P(1A and 1B) atoms and 5.282−5.325 for the 2 P(1C′ and 1D′) atoms, and 1.529−2.181 for the 78 O(1A−35B, O1AL−O4AL, and O1BL−O4BL) atoms and 1.410−2.133 for the 78 O(1C′−35D′, O1C′L−O4C′L, and O1D′L−O4D′L) atoms. These values corresponded to the formal valences of

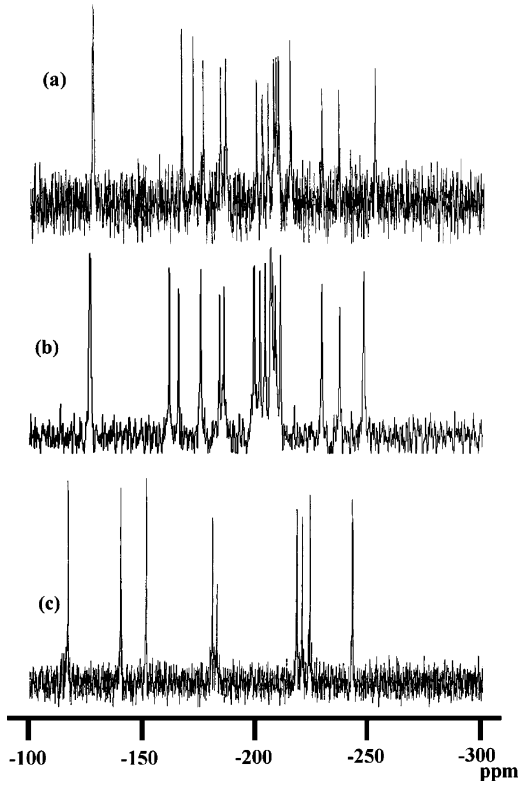

Figure 4. ^{183}W NMR spectra in D_2O of (a) K-**1**, (b) K-**2**, and (c) $[\alpha_2\text{-}P_2W_{17}O_{61}]^{10-}$.

(36) Tourné, P. C. M.; Tourné, G. F.; Brianso, M.-C. *Acta Crystallogr., Sect. B* **1980**, *B36*, 2012−2018.
(37) Brown, G. M.; N.-Spirlet, M.-R.; Busing, W. R.; Levy, H. A. *Acta Crystallogr.* **1977**, *B33*, 1038−1046.

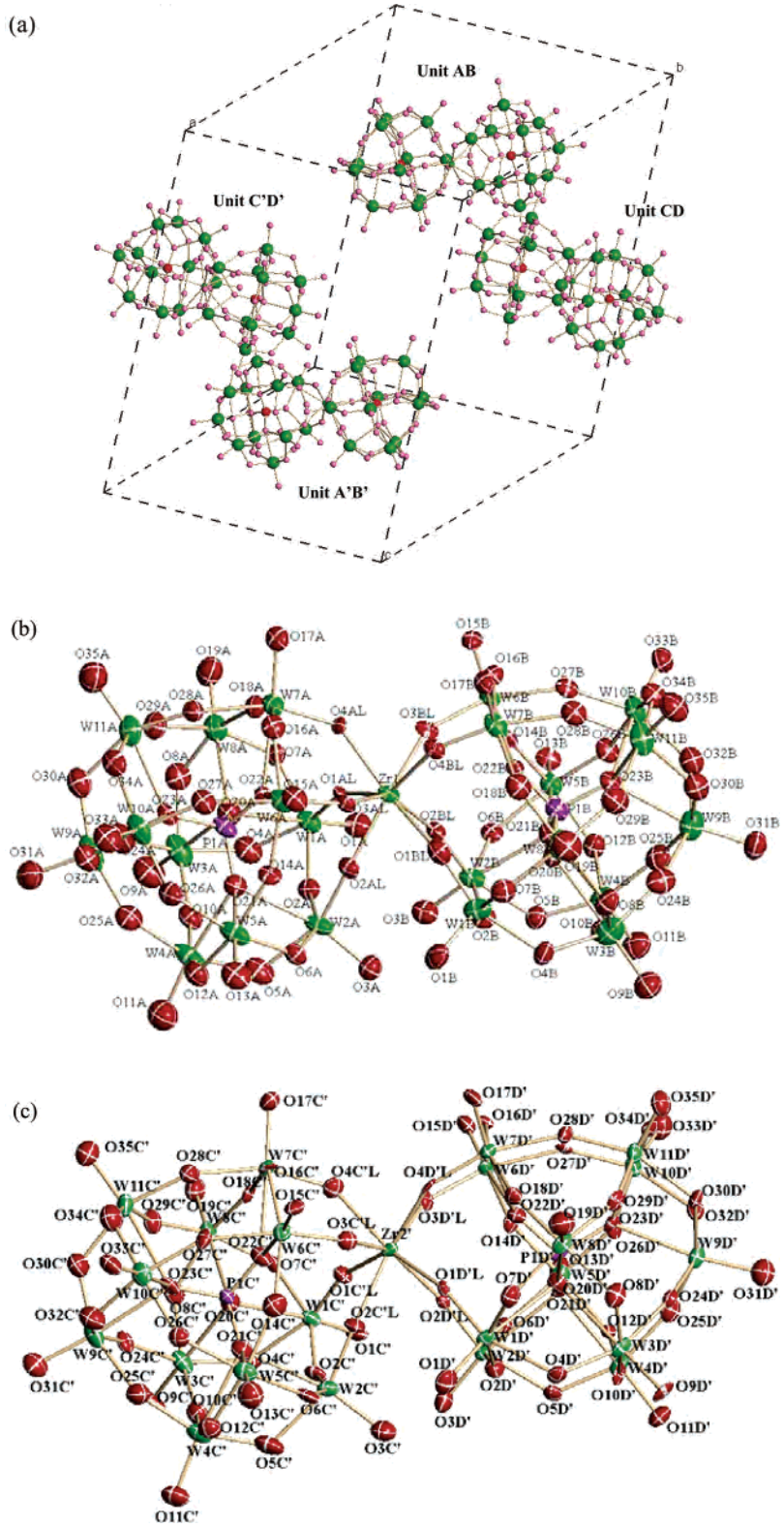

Figure 5. (a) Solid-state packing of the polyoxoanion $[Zr(\alpha\text{-}PW_{11}O_{39})_2]^{10-}$ (**3**) ($Z = 4$). (b, c) Molecular structure of unit AB and C′D′ in **3** with 50% probability ellipsoids, respectively. In (a), units (AB, A′B′) and (CD, C′D′) represent different sets of enantiomeric pairs. The pink, green, red, and small green circles represent the oxygen, tungsten, phosphorus, and zirconium atoms, respectively. In (b) and (c), the molecular structures of units AB and C′D′ are depicted, respectively.

Zr^{4+}, W^{6+}, P^{5+}, and O^{2-}, respectively (Table S9). The BVS values for **4** were 4.022 for the Hf(1) atom and 4.087 for the Hf(2) atom. Further, these values were in the range 5.778−6.519 for the 22 W(1A−11B) atoms and 5.934−6.593 for the 22 W(1C−11D) atoms, 4.788−4.917 for the 2 P(1A and 1B) atoms and 4.965−5.066 for the 2 P(1C and 1D) atoms, and 1.516−2.152 for the 78 O (1A−35B, O1AL−O4AL, and O1BL−O4BL) and 1.533−2.108 for the

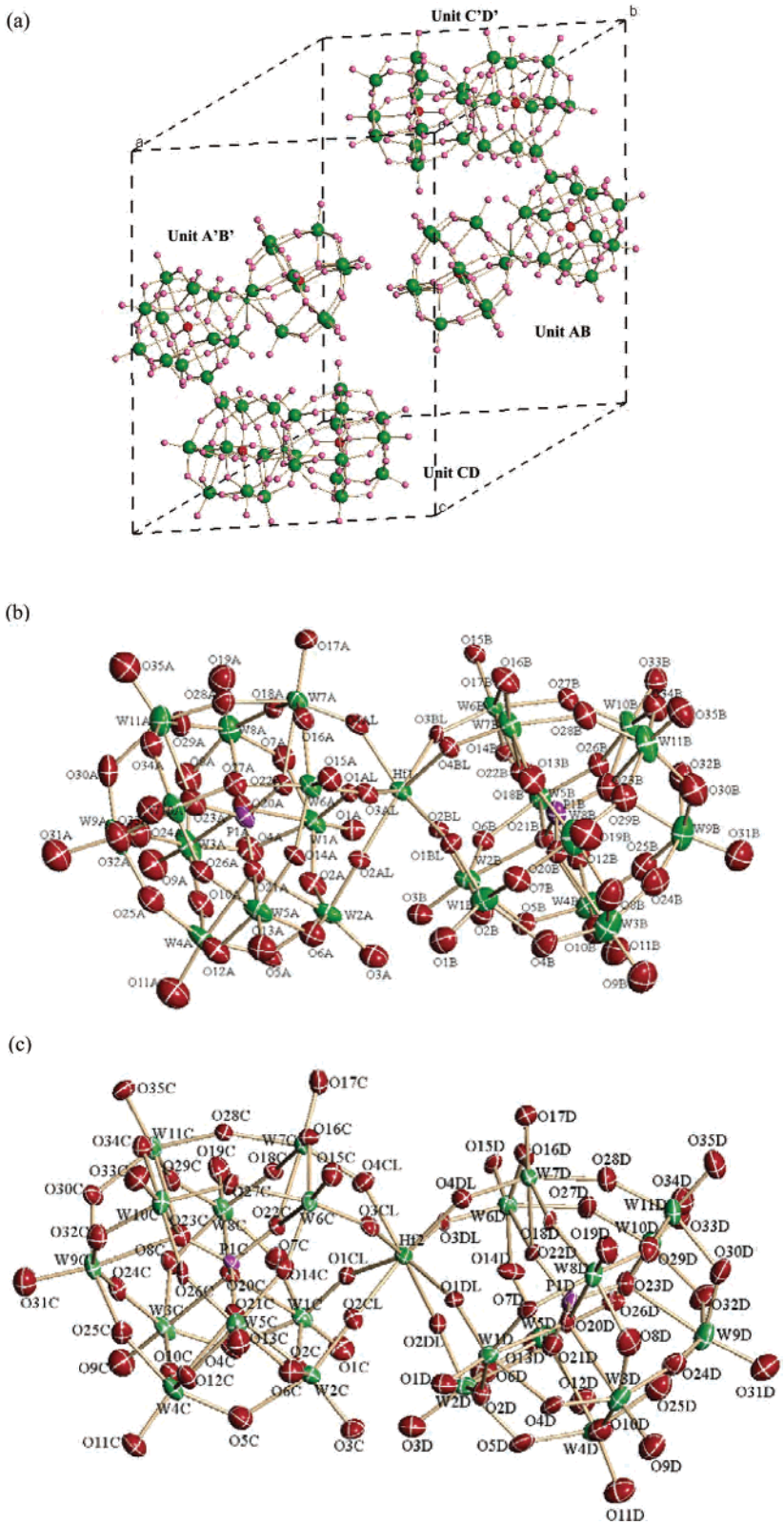

Figure 6. (a) Solid-state packing of the polyoxoanion $[Hf(\alpha\text{-}PW_{11}O_{39})_2]^{10-}$ (**4**) ($Z = 4$). (b, c) Molecular structure of unit AB and CD in **4** with 50% probability ellipsoids, respectively. In (a), units (AB, A′B′) and (CD, C′D′) represent different sets of enantiomeric pairs, respectively. The pink, green, red, and small green circles represent the oxygen, tungsten, phosphorus, and hafnium atoms, respectively. In (b) and (c), molecular structures of the units AB and CD are depicted, respectively.

78 O (1C−35D, O1CL−O4CL, and O1DL−O4DL) atoms. These values corresponded to the formal valences of Hf^{4+}, W^{6+}, P^{5+}, and O^{2-}, respectively (Table S10).

The elemental analyses performed for compounds **3** and **4**, dried at room temperature at 10^{-3}−10^{-4} Torr overnight, were consistent with a composition of $(Et_2NH_2)_{10}[Zr(\alpha\text{-}$

Table 2. Crystal Data for Compounds Et_2NH_2-**3** and Et_2NH_2-**4**

param	Et_2NH_2-**3**	Et_2NH_2-**4**
empirical formula	$C_{40}H_{134}N_{10}O_{85}P_2W_{22}Zr$	$C_{40}H_{124}HfN_{10}O_{80}P_2W_{22}$
fw	6313.43	6310.62
temp (K)	90(2)	90(2)
wavelength (Å)	0.710 73	0.710 73
cryst system	triclinic	triclinic
space group	$P\bar{1}$	$P\bar{1}$
unit cell dimens (Å, deg)	$a = 21.1348(16)$	$a = 21.121(3)$
	$b = 25.5295(19)$	$b = 25.584(3)$
	$c = 25.8012(19)$	$c = 25.835(3)$
	$\alpha = 118.7480(10)$	$\alpha = 118.791(2)$
	$\beta = 91.9300(10)$	$\beta = 91.854(2)$
	$\gamma = 100.8770(10)$	$\gamma = 100.936(2)$
V (Å^3)	11860.3(15)	11888(3)
Z	4	4
D(calcd) (Mg/m^3)	3.536	3.526
abs coeff (mm^{-1})	21.449	22.180
F(000)	11 288	11 216
cryst size (mm^3)	0.21 × 0.04 × 0.01	0.31 × 0.10 × 0.06
θ range for data collcn (deg)	0.91−28.35	0.91−28.36
index ranges	$-28 \le h \le 28$, $-33 \le k \le 34$, $-34 \le l \le 34$	$-27 \le h \le 28$, $-33 \le k \le 34$, $-34 \le l \le 34$
reflcns collcd	159 331	157 401
indpndt reflcns	58 425 [R(int) = 0.1728]	58 494 [R(int) = 0.1064]
refinement method	full-matrix least squares on F^2	full-matrix least squares on F^2
data/restraints/params	58 425/1584/2377	58 494/1506/2260
GOF on F^2	0.959	1.035
final R indices [$I > 2\sigma(I)$]	R1 = 0.0854, wR2 = 0.1923	R1 = 0.0799, wR2 = 0.2077
R indices (all data)	R1 = 0.2160, wR2 = 0.2592	R1 = 0.1486, wR2 = 0.2549
largest diff peak and hole (e•Å^{-3})	8.956 and −5.309	12.718 and −7.221

$PW_{11}O_{39})_2]\cdot 3H_2O$ and $(Et_2NH_2)_{10}[Hf(\alpha\text{-}PW_{11}O_{39})_2]\cdot 0H_2O$, respectively. The weight loss observed during the course of drying before analysis was 1.23% and 0.63%, respectively, which corresponded to 4 and 2 weakly solvated or adsorbed water molecules for **3** and **4**. TG/DTA measurements performed under atmospheric conditions showed a weight loss 1.94% and 0.35%, respectively, which corresponded to the presence of 7 and 2 water molecules due to both intrinsic water of hydration and adsorbed water from the atmosphere. In addition, a weight loss of 11.91% and 11.87% was observed in the temperature range 150−500 °C, respectively, which corresponded to the presence of 10 Et_2NH_2 countercations.

The FTIR spectra of Et_2NH_2-**3** and Et_2NH_2-**4**, which were measured as KBr disks, showed the characteristic vibrational bands of the Keggin-type "$PW_{12}O_{40}^{3-}$" polyoxotungstate framework (Figure S2a,b).[38] Although the P−O bands at 1120 and 1121 cm^{-1} for **3** and **4**, respectively, were shifted from 1080 cm^{-1} of $(Et_2NH_2)_6H[\alpha\text{-}PW_{11}O_{39}]\cdot 3H_2O$, which was prepared by the addition of excess Et_2NH_2Cl to $[\alpha\text{-}PW_{11}O_{39}]^{7-}$, the general spectral patterns in the polyoxoanion regions of **3** and **4** were similar to that of $(Et_2NH_2)_6H[\alpha\text{-}PW_{11}O_{39}]\cdot 3H_2O$ (Figure S2c; 1080 (s), 1041 (s), 950 (vs), 890 (s), 856 (s), 809 (vs), 749 (vs), 620 (m), 591 (m), 508 (m), 432 (w), 410 (w) cm^{-1}). Thus, the structure of $[\alpha\text{-}PW_{11}O_{39}]^{7-}$ was retained after the coordination of Zr and Hf atoms onto the monovacant site of the $[\alpha\text{-}PW_{11}O_{39}]^{7-}$ ligand.

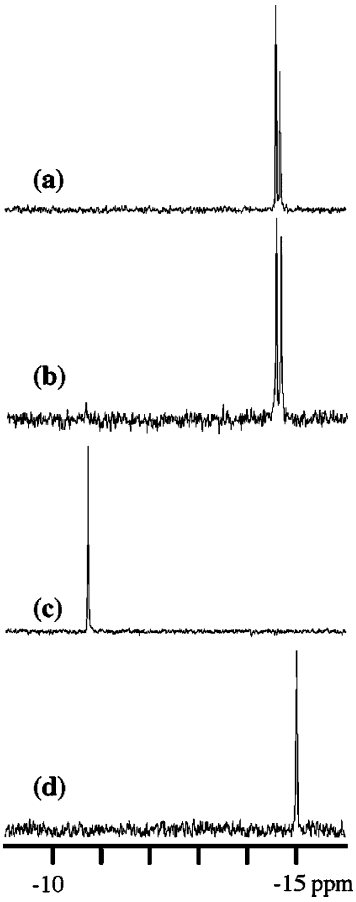

Figure 7. ^{31}P NMR spectra in D_2O of (a) Et_2NH_2-**3**, (b) Et_2NH_2-**4**, (c) $(Et_2NH_2)_6H[\alpha\text{-}PW_{11}O_{39}]\cdot 3H_2O$, and (d) $Na_3[\alpha\text{-}PW_{12}O_{40}]\cdot 11H_2O$.

The ^{31}P NMR spectra of **3** and **4** in D_2O at 25 °C showed a two-line spectrum at −14.57 and −14.65 ppm and −14.67 and −14.77 ppm, respectively, as shown in Figure 7a,b. The

(38) (a) Rocchiccioli-Deltcheff, C.; Thouvenot, R.; Franck, R. *Spectrochim. Acta* **1976**, *32A*, 587−597. (b) Rocchiccioli-Deltcheff, C.; Fournier, M.; Franck, R. *Inorg. Chem.* **1983**, *22*, 207−216. (c) Thouvenot, R.; Fournier, M.; Franck, R.; Rocchiccioli-Deltcheff, C. *Inorg. Chem.* **1984**, *23*, 598−605.

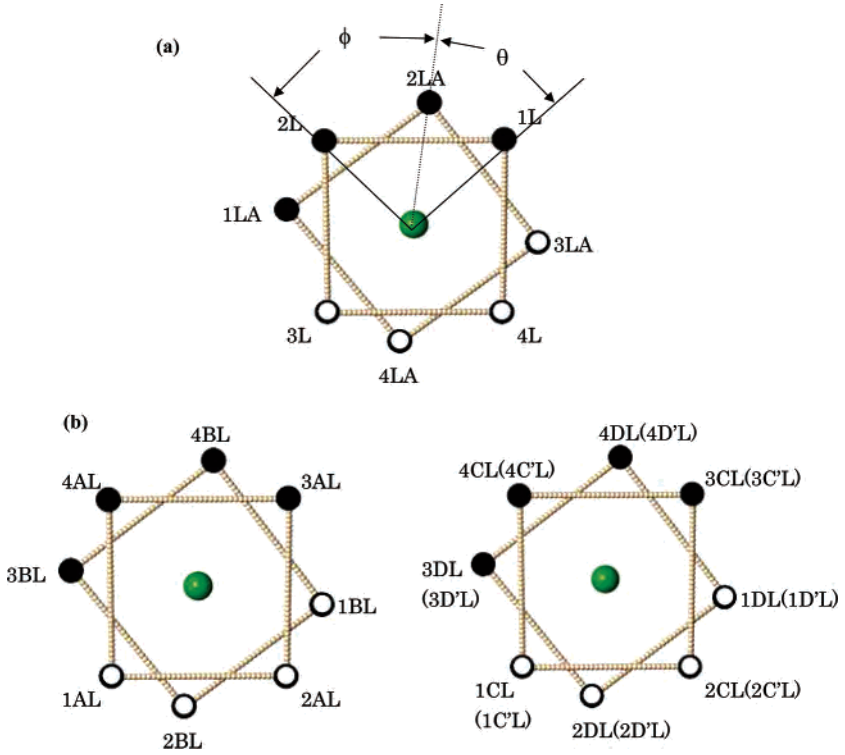

Figure 8. Side view of (a) K-**1** and K-**2** and (b) Et_2NH_2-**3** and Et_2NH_2-**4**. The numbers in parentheses correspond to Et_2NH_2-**3**. The white, black, and green circles represent the terminal oxygen atoms bound to the corner-sharing tungsten atoms, the terminal oxygen atoms bound to the edge-sharing tungsten atoms, and zirconium and hafnium center atoms, respectively.

signals were assigned to the encapsulated phosphorus atom. The two-line spectrum was obtained due to the presence of two units with different bonding modes (bond lengths and bond angles), as determined by X-ray crystallography (Figures 5 and 6). The signals exhibited a shift from those of $[\alpha\text{-}PW_{11}O_{39}]^{7-}$ (Figure 7c; −10.56 ppm) and $[\alpha\text{-}PW_{12}O_{40}]^{3-}$ (Figure 7d; −14.99 ppm), indicating the coordination of Zr and Hf atoms onto the monovacant site of the $[\alpha\text{-}PW_{11}O_{39}]^{7-}$ ligand. The clear ^{183}W NMR spectra of complexes **3** and **4** could not be obtained because of the presence of very close, 22 different signals.

Bonding Modes of Zr and Hf Centers in Complexes 1−4. Figure 8 shows the side view of complexes **1**−**4**. The ϕ and θ in Figure 8 represented the angles O(in the upper plane)−M(Zr, Hf)−O(in the lower plane). The selected bond angles for Dawson and Keggin derivatives are summarized in Tables S11 and S12, respectively. The angle at which $\phi = \theta$ ($|\phi - \theta| = 0$) results in a molecule with a complete square antiprism structure, while $\phi > \theta$ ($|\phi - \theta| > 0$) results in a molecule that is close to a square prism structure rather than a square antiprism structure. The differences between the neighboring O−M−O angles (where M = Zr, Hf) for Dawson and Keggin polyoxoanions **1**−**4** are summarized in Tables S13 and S14. The differences for Zr-coordinated anions **1** and **3** were 1.6−6.1° (average 3.9°) and 5.1−9.6° (6.9°) for Zr(1) and 4.8−6.9° (5.9°) for Zr(2), which were similar to 0.3−5.3° (2.9°) and 6.1−8.2° (7.1°) for Hf(1) and 4.7−5.8° (5.2°) for Hf(2) for Hf-coordinated anions **2** and **4**, respectively, suggesting that the bond angles were hardly influenced by the coordination of Zr and Hf centers. In contrast, the differences between the neighboring O−M−O angles for Dawson polyoxoanions **1** and **2** were significantly smaller than those for Keggin polyoxoanions **3** and **4**, suggesting that the molecular structures of Dawson polyoxoanions **1** and **2** were close to that of a complete square antiprism structure, whereas the square antiprism structures of Keggin polyoxoanions **3** and **4** were distorted to a square prism structure. Thus, the Zr- and Hf-centered structures were influenced by the structure of monovacant sites for the $[\alpha_2\text{-}P_2W_{17}O_{61}]^{10-}$ and $[\alpha\text{-}PW_{11}O_{39}]^{7-}$ ligands. To the best of our knowledge, this is the first example of the comparison of the molecular structures between Dawson and Keggin polyoxoanions with the same metal-centered structures.

Conclusion

A series of zirconium(IV) and hafnium(IV) complexes with Dawson monovacant phosphotungstate $[\alpha_2\text{-}P_2W_{17}O_{61}]^{10-}$ and Keggin monovacant phosphotungstate $[\alpha\text{-}PW_{11}O_{39}]^{7-}$ are presented. We successfully obtained single crystals of water-soluble potassium and diethyammonium salts $K_{15}H[Zr(\alpha_2\text{-}P_2W_{17}O_{61})_2]\cdot 25H_2O$, $K_{16}[Hf(\alpha_2\text{-}P_2W_{17}O_{61})_2]\cdot 19H_2O$, $(Et_2NH_2)_{10}[Zr(\alpha\text{-}PW_{11}O_{39})_2]\cdot 7H_2O$, and $(Et_2NH_2)_{10}[Hf(\alpha\text{-}PW_{11}O_{39})_2]\cdot 2H_2O$ by reacting $ZrCl_2O\cdot 8H_2O$ and $HfCl_2O\cdot 8H_2O$ with monovacant polyanions. The characterization of complexes **1**−**4** was accomplished by X-ray structure analyses, complete elemental analyses, TG/DTA, FTIR, and solution (^{31}P and ^{183}W) NMR spectroscopy. The Zr(IV) and Hf(IV) centers of all the complexes are in a square antipris-

matic coordination environment with eight oxygen atoms, four of them being provided from each of the two monovacant polyanion ligands. The comparison of the bonding modes of the Zr complexes containing Dawson and Keggin polyoxoanions with those of the Hf complexes revealed that (1) the bond lengths of the Zr−O bonds were smaller than those of the Hf−O bonds for both Dawson and Keggin derivatives and the bond length increased with an increase in the ionic radii of the coordinated atoms and (2) the bond angles around the Zr centers were similar to those of the Hf centers for both Dawson and Keggin polyoxoanions. When the bonding modes of the Zr and Hf complexes were compared between Dawson and Keggin polyoxoanions, the differences between the neighboring O−M−O angles around the Zr and Hf centers with Dawson polyoxoanions were found to be smaller than those with Keggin polyoxoanions. This suggests that the molecular structure of Dawson polyoxoanions was close to that of a complete square antiprism structure, whereas the square antiprism structure of Keggin polyoxoanions was distorted to that of a square prism structure. In addition, the average Zr−O and Hf−O bond lengths for Dawson polyoxoanions were smaller than those for Keggin polyoxoanions. Thus, the Zr- and Hf-centered structures were influenced not only by the ionic radii of the coordinated atoms but also by the structure of monovacant sites for Dawson and Keggin polyoxoanion ligands.

Acknowledgment. This work was supported by Grant-in Aid for Scientific Research (C) No. 18550062 and a High-Tech Research Center Project both from the Ministry of Education, Culture, Sports, Science, and Technology of Japan.

Supporting Information Available: X-ray crystallographic files in CIF format and tables of the bond lengths, bond angles, and bond valence sums for compounds K-**1**, K-**2**, Et_2NH_2-**3**, and Et_2NH_2-**4**. This material is available free of charge via the Internet at http://pubs.acs.org.

IC060656E